Chapter 2

Overview on Ion Sensitive Field Effect Transistor and Enzyme FET

2.1 Introduction

In the realm of sensor development, ion sensitive field effect transistor (ISFET) has created a niche for itself as its demand has been increasing in the field of food quality and safety, environmental, medical, military and biotechnology areas etc. With an ever increasing demand in various areas, there is a growing interest for the development of ISFET based sensors which are manufactured by means of semiconductor technology. Middlehock in his review indicated the use of silicon as the substrate in a wide variety of sensors [1]. Wise et al. through their work in the late sixties clearly indicated the capability of the silicon substrate for microelectrodes for electrophysiological measurements [2]. Later, in the year 1970, Piet Bergveld from the University of Twente introduced the concept of ion sensitive field effect transistors in sensor industry and brought about a revolutionary change in pH measurement [3, 4]. The first ISFETs were of silicon dioxide as the sensing membrane and in 1972 the measurement of ionic in and effluxes around a nerve was reported in a work by P.Bergveld [5]. In 1974, Matsuo and Wise also developed a similar device using Si_3N_4 as the sensing sub gate layer which enhanced the performance of the sensor [6]. With these pioneering works, many groups reported several findings on ISFET and its related device.

ISFET are potentiometric sensors and are analogous to its predecessor ion-selective electrodes (ISE). Both ISE and ISFET require an ion-selective membrane as the source of the sensing signal [7]. The main difference between the two is the placement of the membrane; in the ISE the membrane is symmetrically placed between the two solutions whereas for an ISFET the membrane is situated between the sample solution and a solid. A controversy was seen initially regarding the origin of the signal at the interface between the solution and the insulators. One group described this interface as a sheet of pH dependent charge (site binding theory) while the other group considered the pH sensitive region as a hydrated gel layer. A detailed analysis was presented by Sandifer [8] in which the site binding theory was formulated as one extreme of the hydrated gel model. The theoretical data obtained from the model showed that a full Nernstian response depended on the density of protonation sites and on the

thickness of the gel layer thus agreeing to the experimental data obtained for the calculation of pH response. Thus the issue of solution/membrane interface was well understood.

The threshold voltage of an ISFET device is a function of the pH of the electrolyte. The operational mechanism of the ISFET originates from the pH sensitivity of the insulating sensing layer such as SiO_2, Al_2O_3, Si_3N_4 etc. This mechanism is a surface phenomenon which is explained well by site dissociation model [9]. Unlike glass electrodes, ISFET does not need any conditioning period [10]. The response is fully determined by the kinetics of the surface reactions.

Over these several decades, numerous publications appeared which were devoted to various aspects of ISFET development [11]. Few of the latest investigations are related to application of extended gate polycrystalline silicon thin-film transistors to ISFET for the development of DNA hybridization sensors [12], miniaturization of reference electrodes needed for the field effect sensors which is compatible with silicon chip technology [13], integration of ISFET based biosensors with a flow-injection analysis system [14] and development of nanoscale ISFETs [15].

In conventional ion sensor conducting material is used for sensing. Conversely, for an ISFET insulating materials are being used. The only pre-requirement for these sensing materials is that their surface should be able to buffer the ion of interest. In the initial years, not much of importance was given to the fact that the sensing material exhibit Nernstian pH response or not. Later years, lots of researches were done to improve the sensitivity of the pH –ISFET gate. Silicon nitride was reported to have shown better pH response than silicon dioxide [6]. But, it had stability issues. Control and readjustment of the ratio of hydroxyl to amine groups improve the sensitivity [16]. Harame et al. indicated the ratio to be 7/3 to obtain maximum sensitivity [17]. Few methods to improve the sensitivity of silicon nitride were high pressure treatment [18], Rapid Thermal Nitridation [19] and treatment of the surface with 2.45GHz microwave O_2 plasma [20]. Multilayer dielectrics with various insulators such as SiO_2/Si_3N_4 [21], $SiO_2/HfO_2/Al_2O_3$ (OHA) structure [22] had better sensitivity and lower drift rate.

High k dielectric such as HfO_2 [23], Y_2O_3 [24], Pr_2O_3 [25], Er_2O_3 [26] etc. was investigated to be used as the sensing layer to improve the sensitivity. Technique of deposition such as rf sputtering was used to deposit material such as Tungsten Trioxide [27], Aluminum Nitride [28] etc. which affects the sensitivity of the device. In addition to these, techniques were employed such as biasing conditions, electrostatic screening, inner metal dielectric overlying external gate to name a few. Improved sensitivity was obtained for FET based biosensors when biased in sub threshold regime [29].Decreasing Debye Huckel (DH) screening too resulted in better sensitivity [30]. Hence, structures with engineered bias conditions were introduced to improve pH sensitivity. Techniques such as IMD technology which utilizes a remote gate in the device comprising of polysilicon/aluminum with sensing membrane layer of IMD overlying the extended gate resulted into a significant improvement in chemical sensitivity and effective transconductance [31]. Besides these, few other structures such as dual gate (DG) ISFET using capacitive coupling[32], addition of second gate (a Self-Assembled Monolayer) (SAM) layer [33], Suspended gate Field Effect Transistors (SGFET) [34] etc. were proposed to breach Nernst limit of 59mV/pH .

In recent times, improvement in ISFET fabrication has been highly influenced by the advances in microelectronic technologies. The encapsulation of the ISFET based sensors is very critical [35]. Precaution measures are to be taken as such that the gate area alone remains in contact with the liquid. Manual methods such as thermosetting resins were generally used which lowered manufacturing reproducibility and increased cost. A new alternative has been proposed by Bratov et al. for an automated method of encapsulation by the use of photocurable polymer [36]. Exposure to UV helps to pattern the polymer layers with the help of standard mask aligner thus resulting in semi-automation of the encapsulation process.

Although the history of ISFET dates back to seventies, commercialization of probes with ISFETs started only in the nineties. This is mainly because of some constraints due to inherent problems such as drift, temperature and light sensitivity, and technological limitations such as encapsulation and the need for a stable miniaturized reference electrode. Some of the commercially available pH

ISFET are from companies such as ThermoORION (USA), Sentron (NL), Microsens S.A. (CH), Honeywell (USA), D+T Microelectronica (SP).

Initially, the research went in the direction of ion sensing in general, it was only after a decade its biomedical aspect was explored. Devices where ISFET were used in conjunction with some biological material resulted into a device known as bioFETs, which is a transistor device with a bio-sensitive layer that can specifically detect bio-molecules such as nucleic acids and proteins. Different types of biological sensitive material include either biological molecules species such as enzymes, multi-enzyme systems, antibodies, antigens, proteins, or nucleic acids or living biological systems such as cells, plant tissue slices, intact organs or whole organisms which uses biochemical mechanisms for recognition. The biological recognition system translates the information from the bio-chemical domain, typically an analyte concentration, into a bio-chemical response. Due to the molecular interactions, one or more physico-chemical parameters changes which produce ions, electrons, gasses, heat or light, etc. These quantities are converted into electrical signal by the transducer part, which is further amplified, processed and displayed in a suitable form. Enzyme, a bioreceptor, has a specific binding ability. The idea of ENFET was proposed by Janata and Moss in 1976 [37] and the first EnFET was realized by Caras and Janata in 1980 where penicillinase (penicillin hydrolyzing enzyme) was immobilized on the ISFET sensor [38]. In the later years, a large magnitude of ENFETs differing in sensor design or gate material , enzyme membrane composition or immobilization method have been reported for detection of the analytes such as glucose, urea, penicillin, ethanol, lactose, sucrose, maltose, ascorbic acid, lactase, acetylcholine, organophosphorus pesticides, formaldehyde, creatinine, etc[39-49].

Some of the practical applications of ENFETs includes determination of glucose in blood serums [50] and urine [51], urea in blood serum [52, 53] and in hemodialysis fluids [54], creatinine in hemodialysis solutions and in serum of renal failure patients [55], vitamin C in beverages [56]. An ENFET array integrated into a commercial flow-injection system [57] were utilized to monitor glucose, maltose, sucrose, lactose, ethanol, and urea concentrations during the cultivation of *Escherichia coli* and *Saccharomyces cerevisiae*. Penicillin sensitive

ENFETs were used for determination of penicillin G in penicillin fermentation broths [58].

The following sections in this chapter give in brief the theory of ISFET which include the development of ISFET encompassing the site binding and electrical double layer concept. The later section deals about the EnFET and the principle behind it.

2.2 Theory on ISFET

The ISFET can be understood well if an analogy is drawn with the Metal oxide semiconductor field effect transistor (MOSFET). Therefore, all works on ISFET always start with the explanation of the theoretical concept of MOSFET to explain the operation mechanism of ISFET. The ISFETs are devoid of the gate layer present in MOSFETs and the device when introduced in the electrolyte, the solution comes in direct contact with the sensing layer. The figure 2.1 illustrates an ISFET device. The gate circuit is completed by the presence of a reference electrode immersed in the solution [59].

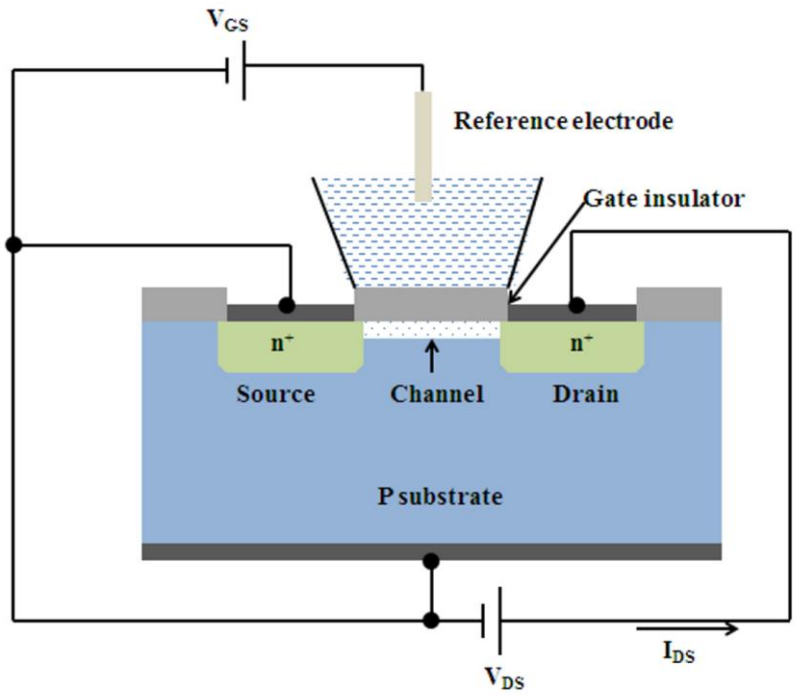

Figure 2.1. Figure depicting the schematic of ISFET device

The sensing membrane in the device can buffer the ion of interest of the electrolyte solution. The threshold voltage which indicates the onset of drain current, for a MOSFET comprises of voltages due to surface potential, work function difference between the metal and the semiconductor and the charges trapped in the oxide layer [59, 60].

$$V_{th(MOSFET)} = 2|\phi_f| + \phi_m - \phi_{si} - \frac{Q_{ox} + Q_{ss} + Q_B}{C_{ox}} \qquad (2.1)$$

Here ϕ_f is fermi potential of the semiconductor

ϕ_m and ϕ_{si} is the work function of the metal and semiconductor respectively

Q_{ox} is accumulated oxide charges

Q_{ss} is the fixed surface state charge per unit area at the insulator semiconductor interface,

Q_B is the depletion charge in the silicon per unit area

C_{ox} is the oxide capacitance per unit area

In case of an ISFET, the same fabrication process can be used that may result into same constant parameters of the threshold voltage as in equation (2.1). However, in ISFET the presence of electrolyte, its direct contact with the sensing layer few additional parameters are also present. The expression for the threshold voltage of an ISFET is given as [60]

$$V_{th(ISFET)} = E_{ref} + \phi_{lj} - \phi_{eo} + \chi_{sol} - \phi_{si} - \left(\frac{Q_{ox} + Q_{SS} + Q_B}{C_{ox}}\right) + 2\phi_f \qquad (2.2)$$

Here E_{ref} is the potential of the reference electrode and is a constant

Φ_{eo} is the interfacial insulator/electrolyte potential which is a function of the pH of the solution

χ_{sol} is the surface dipole potential of the solvent and is a constant

Φ_{lj} is the liquid junction potential difference between the reference solution and the electrolyte

The threshold voltage of an ISFET can further be written in terms of a MOSFET as [60]

$$V_{th(ISFET)} = V_{th(MOSFET)} + E_{ref} + \phi_{lj} + \chi_{sol} - \phi_{eo} - \phi_m \tag{2.3}$$

The general expression for the drain current in ohmic region of the MOSFET and also applicable for ISFET is [60]

$$I_{DS} = \beta\left((V_{GS} - V_{th})V_{DS} - \frac{V_{DS}^2}{2}\right) \tag{2.4}$$

For the saturated region, the expression is [60]

$$I_{DS} = \frac{\beta}{2}(V_{GS} - V_{th})^2 \tag{2.5}$$

Here, β is the device transconductance parameter which is depended on the mobility (μ), gate insulator capacitance C_{ox} and the aspect ratio or width to length ratio. The expression of β is given as

$$\beta = \mu C_{ox}\frac{W}{L} \tag{2.6}$$

The working of an ISFET can be explained by two theory- site binding theory and electrical double layer theory.

2.2.1 Site binding theory

In 1974, Yates et al. described the site binding model for silicon dioxide surface [61]. The model explains the mechanism of establishing the equilibrium between the charges in the oxide layer and the ions present in the electrolyte. The oxide layer is assumed to be amphoteric i.e. the surface hydroxyl groups are neutral, protonated or deprotonated depending on the pH of the bulk solution. At lower pH values the protonated groups predominate and at higher pH values the deprotonated groups predominate. The site binding theory is illustrated in figure 2.2 for silicon dioxide layer.

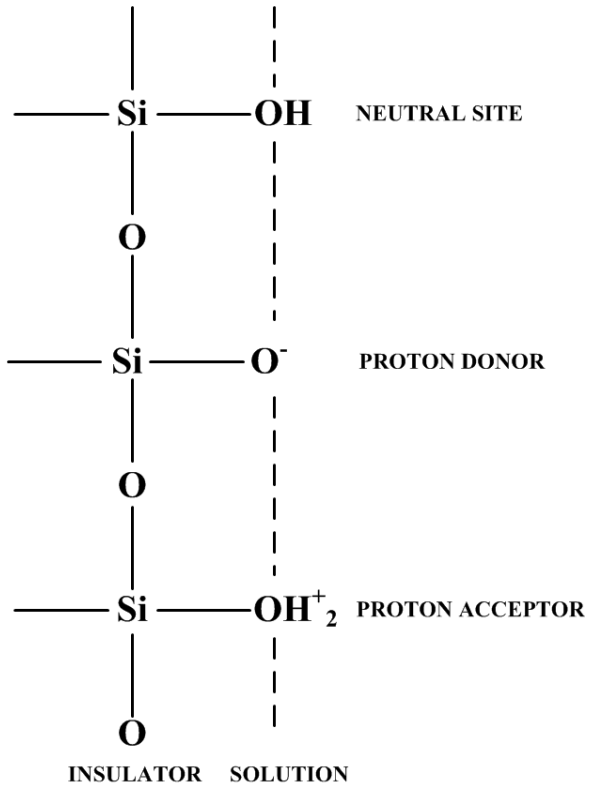

Figure 2.2 Schematic representation of site binding model

2.2.2 Electrical double layer

The exchange of hydrogen ions between the surface groups and electrolyte brings about a change in the charges at the electrolyte insulator interface. The active sites are formed by the interaction with the protons and the surface groups. The redistribution of charges results into a change in the potential at the interface. This forms the electrical double layer.

There are three theoretical treatments of the double layer on the interface, Helmholtz Plane Theory, Gouy-Chapman Theory, and Gouy-Chapman Stern Model. The Helmholtz Double Layer theory (1879) is a simple approximation in which the surface charge is neutralized by counter ions of opposite sign [60]. The charge in the solution is located at the Outer Helmholtz plane (OHP) and the surface is treated as a parallel plate capacitor. However, since this model hypothesizes rigid layers of opposite charges, this does not occur in nature. Therefore, Gouy-Chapman double layer theory (1910-1913) was introduced in addition to the Helmholtz Double Layer theory [62] . Here, the counter ions are not rigidly held, but they tend to diffuse into the liquid phase until a counter

potential restricts this tendency. The ion concentration distribution in the diffusion layer is given by a Boltzmann equation [63]. The assumption that only oppositely charged ions diffuse into the bulk solution contradicts the double layer thickness found experimentally and the calculated one. This is because not only the oppositely charged ions but also same sign charges as that of surface charges too will be found within the double layer. Therefore, the third model i.e. inclusion of a Stern layer into the existing theory was done. Thus the electrical double layer is explained well by Gouy Chapman Stern theory [64, 65, 66, 67].

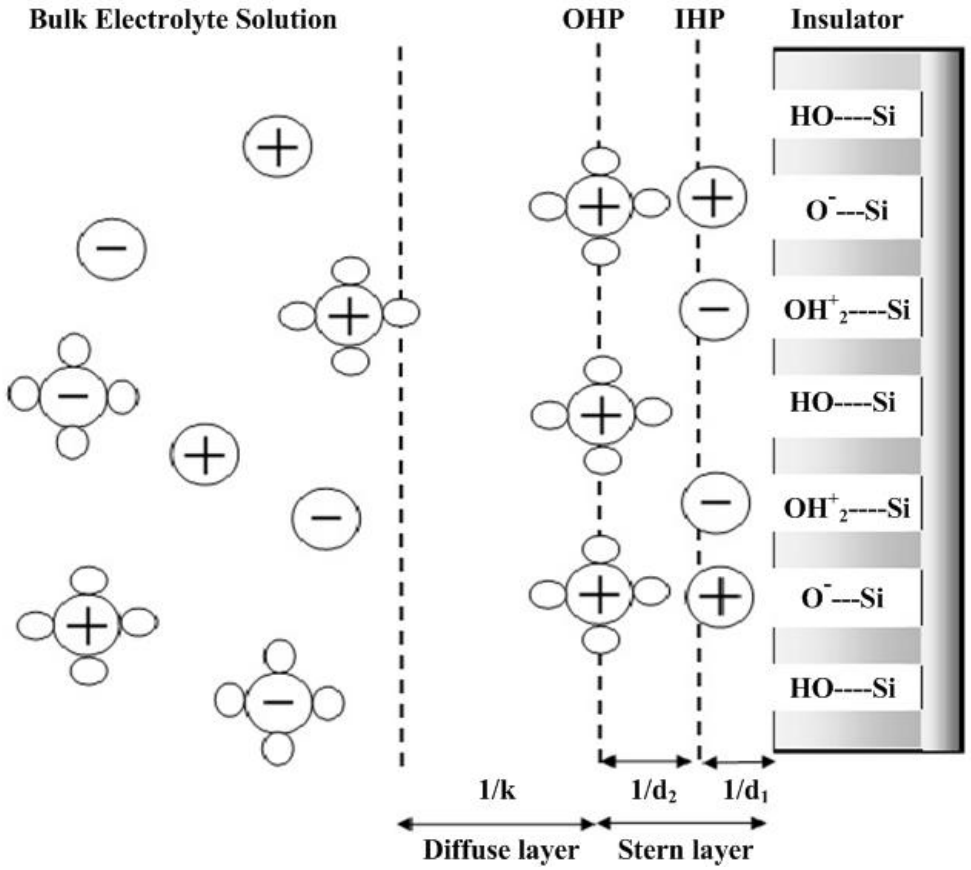

Figure 2.3. The Stern and Gouy –Chapman layers in an electrical double layer

Various parts of the electrical double layer are depicted in figure 2.3. Further, the charge distribution and potential profile of an Electrolyte Insulator Semiconductor (EIS) system are illustrated in figure 2.4(a) for $pH>pH_{PZC}$ and (b) for $pH<pH_{PZC}$ [68].

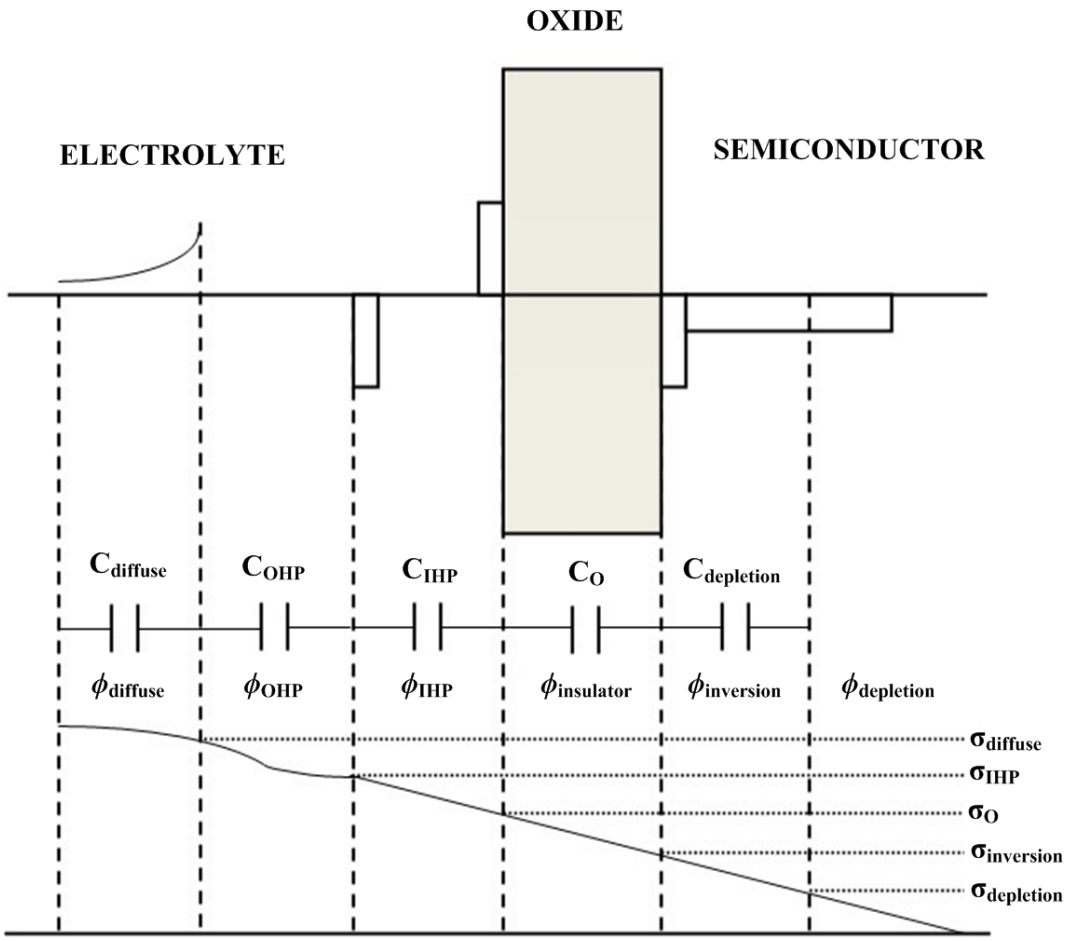

Figure 2.4(a) Charge distribution and potential profile of an EIS system for pH> pH_{PZC}

The symbols used to illustrate the EIS system are:-

C_o	Capacitance of the oxide layer	$\phi_{inversion}$	Potential across the inversion layer
$C_{diffuse}$	Capacitance of the diffuse layer	$\phi_{depletion}$	Potential across the depletion layer
C_{OHP}	Capacitance of the OHP layer	$\sigma_{diffuse}$	Charge in the diffuse layer
C_{IHP}	Capacitance of the IHP layer	σ_{IHP}	Charge in the IHP layer
$C_{depletion}$	Capacitance of the semiconductor layer	σ_o	Surface charge
$\phi_{diffuse}$	Potential across the diffuse layer	$\sigma_{inversion}$	Charge in the inversion layer
ϕ_{OHP}	Potential across the OHP layer	$\sigma_{depletion}$	Charge in the depletion layer
ϕ_{IHP}	Potential across the IHP layer		

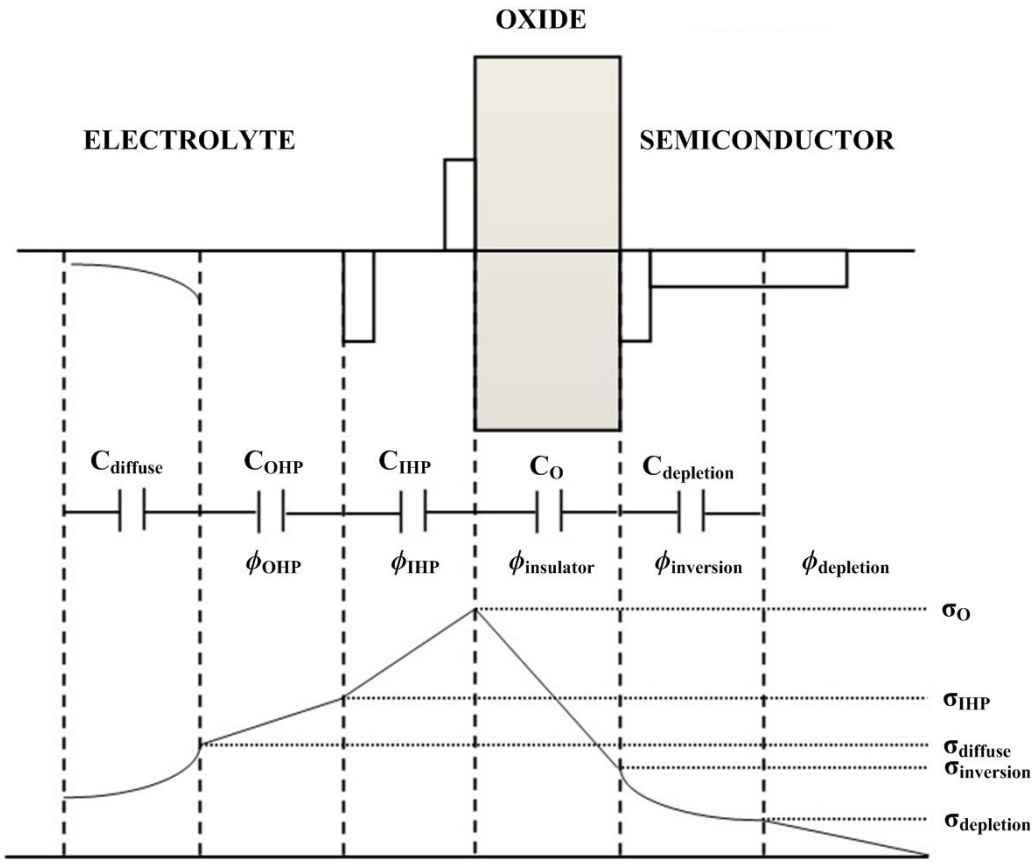

Figure 2.4(b) Charge distribution and potential profile of an EIS system for pH< pH_{PZC}

The Gouy Chapman Stern theory states that the double layer formed at the vicinity of the sensing layer is divided into two parts: Stern layer and Gouy Chapman diffuse layer. The adsorbed ions at the immediate vicinity of the interface form the Stern layer. The Stern layer is divided into Inner Helmholtz Plane (IHP) and the Outer Helmholtz Plane (OHP). The inner part of the Stern layer is the IHP and it passes through the center of the counter ions specifically adsorb on the interface. Next to the IHP is the OHP which passes through the centers of the next layer of non-specifically adsorbed ions. The potential drop in these two layers is linear and is sharper in the inner layer than the outer layer. Beyond OHP is the diffuse layer which is known as the Gouy Chapman layer. The point in the diffuse layer until which the effect of the sensing layer is felt by the ions in the electrolyte is called the Debye length which is represented by *1/k (in this thesis it is represented as L_D in later chapters*). *k* is known as Debye Huckel parameter. The electrical double layer can be assumed to be two parallel plate

capacitors, C_H and C_D in series. C_H is the Helmholtz capacitance and C_D is the diffused layer capacitance. The Helmholtz plane is further divided into the C_{IHP} and C_{OHP}.

In 1980, Bousse et al. used the site binding model for the EIS surface and proved that it could be used for ISFET surfaces of SiO_2 and Al_2O_3 [9]. Both the site binding and electrical double layer theory concepts were used and two parameters were developed. One is pH_{PZC} which is the value of the pH at which the surface is electrically neutral. The other is the sensitivity represented as β. The resulting equation is the surface potential equation which is given as [9]

$$\phi_{eo} = 2.3\frac{KT}{q}\frac{\beta}{\beta+1}\left(pH_{pZC} - pH\right) \tag{2.7}$$

Equation (2.7) clearly indicates that the surface potential is dependent on the sensitivity and lower value of it can lead to sub-Nernstian range. Further, the proton concentration at the surface can be related to the concentration at the bulk by Boltzmann statistics. The group of Grattarola used this parameter as a mathematical quantity after associating it with the site dissociation model and gave the PSPICE model for different types of surface sites [69]. The significance of the $[H^+]_S$ was put forward later in a work reported by Hal and Eijkel [70, 71, 72]. The well-known electrical equation of $Q=CV$ was used for comparison of the acid base model of a protein molecule. Q indicated the surface charge which are the protonized or deprotonized groups of the oxide surface, C indicated the electrical double layer capacitance at the interface and the V denoted the resulting surface potential i.e. ϕ_{eo} . The final value of the surface potential ϕ_{eo} was given by an equation with a sensitivity factor α stated as [72, 73]

$$\Delta\phi_{eo} = -2.3\,\alpha\frac{RT}{F}\Delta pH_{bulk} \tag{2.8}$$

Where α is given as

$$\alpha = \frac{1}{(2.3kT/q^2)(C_s/\beta_s)+1} \tag{2.9}$$

Here β_S is the surface buffer capacity and it is the capacity of the oxide surface to consume or deliver hydrogen ions and C_S is the differential double layer capacitance. The dimensionless parameter α should lie between 0 and 1 and is dependent on the intrinsic buffer capacity and the differential capacitance.

Maximum sensitivity can be achieved if the intrinsic buffer capacity is high. Maximum Nernstian sensitivity can be achieved if α approaches unity and sub Nernstian value is attained if it is lesser than unity. α becomes equal to unity with high surface buffer capacity β_s and low double layer capacitance C_s. Therefore, ISFET, which is similar to MOSFET, the prior's threshold voltage can be modulated by means of the interfacial potential of the oxide and the electrolyte. The buffer capacity of the oxide surface determines the relation between the interface potential and the pH. In conventional ion sensor, only conducting material is used whereas in ISFET insulating materials are being used. The only pre-requirement for these sensing insulators is that their surface should be able to buffer the ion of interest [9].

2.3 ISFET modeling

Modeling of ISFET predicts the function of the device for different sensing layer which enhances the sensitivity. In all the models whether based on physico- chemical or Simulation Program with Integrated Circuit Emphasis (SPICE) the basic objective is to obtain a relation between the interfacial electrode electrolyte potential and the pH of the electrolyte [73]. This section describes, in brief, some mathematical quantities used for the ISFET models. Here the modeling is shown for silicon dioxide surface, therefore, the positive, negative and neutral surface site is denoted as $SiOH^{+}_{2}$, SiO^{-} and SiOH respectively. Exchange of the hydrogen ions with these sites can be expressed as follows [60, 74]

$$SiOH \xleftrightarrow{K_a} SiO^{-} + H_s^{+} \tag{2.10}$$

$$SiOH + H_s^{+} \xleftrightarrow{K_b} SiOH_2^{+} \tag{2.11}$$

Under equilibrium conditions, the dissociation constants are expressed as

$$K_a = \frac{[\mathrm{SiO^-}][\mathrm{H_S^+}]}{[SiOH]} \tag{2.12}$$

$$K_b = \frac{[\mathrm{SiOH_2^+}]}{[SiOH][\mathrm{H_S^+}]} \tag{2.13}$$

s in the subscript indicates proton concentration at the surface. Combining equation (2.12) and (2.13)

$$\left[H^+\right]_S = \sqrt{\frac{K_a[SiOH_2^+]}{K_b[SiO^-]}} \tag{2.14}$$

Considering the surface to be neutral i.e. when $[SiOH^+_2] = [SiO^-]$ equation (2.14) becomes

$$\left[H^+\right]_S = \sqrt{\frac{K_a}{K_b}} \tag{2.15a}$$

Taking logarithm on both sides of above equation

$$\ln\left[H^+\right]_S = \ln\sqrt{\frac{K_a}{K_b}} \tag{2.15 b}$$

$$\text{Where } -\ln\left(\frac{K_a}{K_b}\right)^{\frac{1}{2}} = -2.303\log\left(\frac{K_a}{K_b}\right)^{\frac{1}{2}} = 2.303\,pH_{PZC} \tag{2.16}$$

pH_{PZC} point of zero charge is the value of pH for which the surface is electrically neutral. Further, the proton concentration at the surface is related to bulk concentration by Boltzmann distribution.

$$\left[H^+\right]_S = \left[H^+\right]_{bulk} \exp\left(\frac{-q\phi_{eo}}{KT}\right) \tag{2.17}$$

This surface potential ϕ_{eo} is generated by the net surface concentration charge expressed as [60]

$$\sigma_o = q\left(\left[SiOH_2^+\right]-\left[SiO^-\right]\right) \tag{2.18}$$

The total number of surface sites is given by

$$N_S = \left[SiOH\right]+\left[SiO^-\right]+\left[SiOH_2^+\right] \tag{2.19}$$

Considering equation (2.12, 2.13, 2.18 and 2.19) the surface charge density is expressed as

$$\sigma_o = q\times N_S\frac{[H^+]_S^2 - K_aK_b}{[H^+]_S^2 + K_a[H^+]_S + K_aK_b} \tag{2.20}$$

The relation between pH of a solution, surface potential ϕ_{eo} and surface charge density can be established by the equations (2.10-2.13, 2.17-2.19) [75]

$$[H^+] = \left(\frac{K_a}{K_b}\right)^{1/2}\exp(y_o)\frac{\left[\frac{\alpha_o}{\delta}+1+\left(\frac{\alpha_o}{\delta}\right)^2\left(1-\delta^2\right)\right]^{1/2}}{1-\alpha_o} \tag{2.21}$$

Here, $y_o = q\phi_{eo}/KT, \alpha_o = \sigma_o/qN_S$ and $\delta = 2(K_aK_b)^{1/2}$. The parameter δ was introduced by Healy et al. [76] and it characterizes the reactivity of the insulator surface. For oxides, $\delta<<1$ and consequently putting 1- $\delta^2\approx1$ in equation 2.21 the expression obtained is

$$[H^+] = \left(\frac{K_a}{K_b}\right)^{1/2}\exp(y_o)\frac{\left[\frac{\alpha_o}{\delta}+1+\left(\frac{\alpha_o}{\delta}\right)^2\right]^{1/2}}{1-\alpha_o} \tag{2.22}$$

Now, if considered y_o= 0, α_o=0 then equation 2.15 is obtained. Taking logarithm on both sides of the equation (2.22)

$$\ln[H^+] = \ln\left(K_a/K_b\right)^{1/2} + y_o + \ln\left[\frac{\alpha_o}{\delta} + 1 + \left(\frac{\alpha_o}{\delta}\right)^2\right]^{1/2} - \ln(1-\alpha_o)$$

$$\ln[H^+] - \ln\left(K_a/K_b\right)^{1/2} = y_o + \sinh^{-1}\left(\frac{\alpha_o}{\delta}\right) - \ln(1-\alpha_o) \tag{2.23}$$

Substitution equation (2.16) in equation (2.23), the expression obtained is

$$2.303\left(pH_{PZC} - pH\right) = y_o + \sinh^{-1}\left(\frac{\alpha_o}{\delta}\right) - \ln(1-\alpha_o) \tag{2.24}$$

The last term in equation (2.24) can be neglected for silicon dioxide surface. Hence the expression becomes

$$2.303\left(pH_{PZC} - pH\right) = y_o + \sinh^{-1}\left(\frac{\alpha_o}{\delta}\right) \tag{2.25}$$

According to Gouy Chapman Stern theory, insulator electrode interfacial potential is the summation of the potential across the Stern layer and the diffuse layer. Therefore, the expression is given as

$$\phi_{eo} = -2(\mathrm{KT/q})\sinh^{-1}\left(\frac{\sigma_{diffuse}}{(8\varepsilon_{diffuse}KTC_{conc})^{1/2}}\right) - \frac{\sigma_{diffuse}}{C_H} \tag{2.26}$$

$\varepsilon_{diffuse}$ is the dielectric constant of the diffuse layer , C_{conc} is the concentration of the electrolyte , $\sigma_{diffuse}$ is the charge in the diffuse layer.

For small values, diffuse layer can be written as

$$\phi_{eo} = -2(\mathrm{KT/q})\left(\frac{\sigma_{diffuse}}{(8\varepsilon_{diffuse}KTC_{conc})^{1/2}}\right) - \frac{\sigma_{diffuse}}{C_H} \tag{2.27}$$

$$\phi_{eo} = -\frac{\sigma_{diffuse}}{C_D} - \frac{\sigma_{diffuse}}{C_H} \tag{2.28a}$$

$$\phi_{eo} = -\frac{\sigma_{diffuse}}{C_d} \tag{2.28b}$$

Here, $\frac{1}{C_d} = \frac{1}{C_D} + \frac{1}{C_H}$

Therefore, diffuse layer capacitance (C_D) is given as

$$C_D = -\frac{d\sigma_{diffuse}}{d\phi_{eo}} \approx \left(\sqrt{8\varepsilon_o\varepsilon_r KTC_{conc}}\right)\left(\frac{zq}{2KT}\right) \tag{2.29}$$

In absence of applied voltage to the reference electrode, the diffuse layer charge is given as

$$\sigma_{diffuse} = -\left(\sqrt{8\varepsilon_o\varepsilon_r KTC_{conc}}\right)\sinh\left(\frac{zq\phi_{eo}}{2KT}\right) \approx -\left(\sqrt{8\varepsilon_o\varepsilon_r KTC_{conc}}\right)\left(\frac{zq\phi_{eo}}{2KT}\right) \tag{2.30}$$

Stern plane is further divided into IHP and OHP, hence the capacitance is expressed as

$$C_H = \frac{1}{\frac{1}{C_{IHP}} + \frac{1}{C_{OHP}}} \tag{2.31}$$

$C_{IHP} = \frac{\varepsilon_{IHP}}{t_{IHP}}$ and $C_{OHP} = \frac{\varepsilon_{OHP}}{t_{OHP}}$

Here, t_{IHP} and t_{OHP} represents the thickness of the IHP and OHP layer respectively.

From the viewpoint of charge neutrality, as shown in figure 2.4(a) and 2.4(b) the charge density and the potential profile of an EIS system

$$\sigma_{diffuse} + \sigma_{IHP} + \sigma_{OHP} + \sigma_{insulator} + Q_{semiconductor} = 0 \tag{2.32}$$

$$Q_{inversion} + Q_{depletion} = Q_{semiconductor} \tag{2.33}$$

$$\sigma_{IHP} + \sigma_{OHP} + \sigma_{insulator} = \sigma_o \tag{2.34}$$

Substituting equation (2.33) and (2.34) in equation (2.32) is given as

$$\sigma_{diffuse} + \sigma_o + Q_{inversion} + Q_{depletion} = 0 \tag{2.35}$$

In absence of any applied voltage, inversion charge is zero and depletion charge is negligibly low. Therefore, equation (2.35) can be written as

$$\sigma_{diffuse} + \sigma_o = 0$$

$$\sigma_{diffuse} = -\sigma_o \tag{2.36}$$

Again rewriting equation (2.25) with α_o and δ terms replaced the equation obtained is

$$2.303(pH_{PZC} - pH) = y_o + \sinh^{-1}\left(\frac{\sigma_o}{2qN_S\left(K_aK_b\right)^{1/2}}\right) \tag{2.37}$$

$$\sigma_{diffuse} = -C_d\phi_{eo} \tag{2.38}$$

Substituting equation (2.38) in equation (2.37)

$$2.303(pH_{PZC} - pH) = y_o + \sinh^{-1}\left(\frac{C_d\phi_{eo}/qN_S}{2\left(K_aK_b\right)^{1/2}}\right) \tag{2.39}$$

Substituting the value of ϕ_{eo} in terms of y_o in equation (2.39) and rearranging the terms, the expression obtained is

$$2.303(pH_{PZC} - pH) = y_o + \sinh^{-1}\left(\frac{y_o}{\frac{q^2N_S2\left(K_aK_b\right)^{1/2}}{KTC_d}}\right) \tag{2.40}$$

$$2.303(pH_{PZC} - pH) = y_o + \sinh^{-1}\left(\frac{y_o}{\beta}\right) \tag{2.41}$$

Where $\beta = \frac{q^2 N_S 2(K_a K_b)^{1/2}}{KTC_d}$ is a dimensionless parameter which indicates the sensitivity.

Replacing the terms of y_o and considering $y_o << \beta$ the equation (2.41) can be written as [9]

$$\phi_{eo} = 2.303 \frac{KT}{q}(pH_{PZC} - pH)\frac{\beta}{1+\beta} \tag{2.42}$$

Therefore equation (2.42) relates interfacial insulator electrolyte potential with the buffer sensitivity.

2.4 Enzyme Field Effect Transistor

It is already mentioned that ISFET when used in conjunction with biological element such as enzyme results into a bio-electronic device called Enzyme Field Effect Transistor. It belongs to the class of potentiometric sensors which has high selectivity and sensitivity [77]. In 1962 first electrode based biosensor was developed by Clarke [78] and the first ENFET was realized in 1980 [38].

An ENFET is constructed by immobilizing an enzyme on the insulator layer of the ISFET. The immobilizing technique can involve a various number of methods- such as physical or chemical adsorption, entrapment within polymeric matrices, covalent binding, cross-linking by bi-functional crosslinking agents (such as glutaraldehyde) and mixed physicochemical methods (entrapment and cross-linking) [10, 39, 79, 80, 81]. Figure 2.5 illustrates the structure and the functional principle of a penicillin-sensitive ENFET [82].

In an enzymatic reaction there are mainly three components the enzyme, substrate or analyte and the product, where analyte is converted to product in a single substrate enzyme catalytic reaction. In context with consumption or production of protons (H^+) in an enzymatic reaction the change in the concentration can be monitored by the underlying ISFET. Hence, a change in the ISFET signal can be correlated with the original analyte concentration.

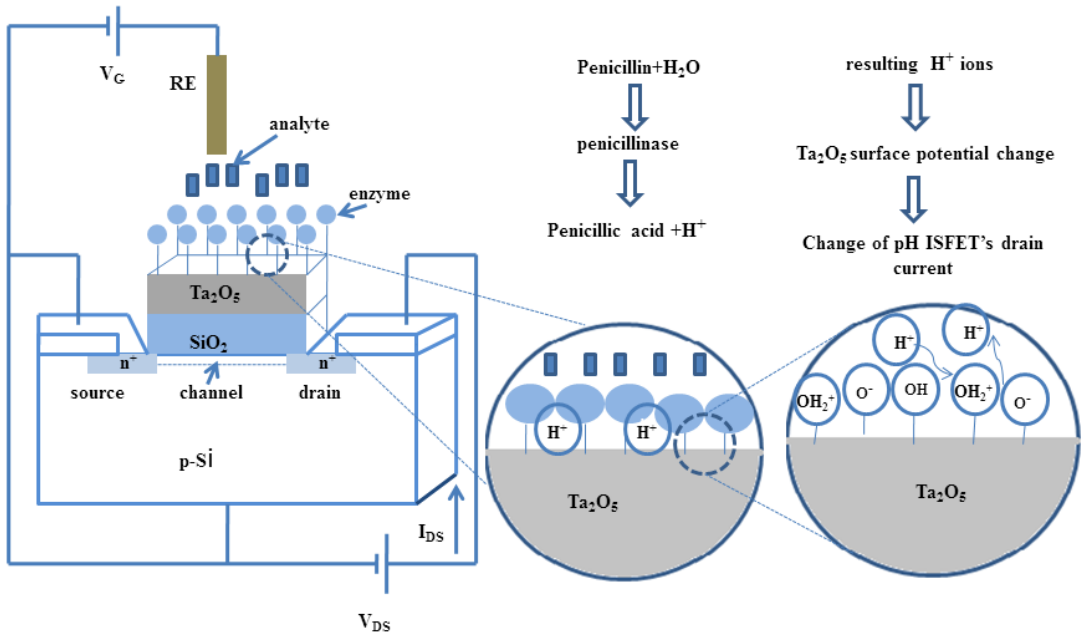

Figure 2.5 Figure depicting the structure and functional principle of a penicillin sensitive ENFET (RE- Reference Electrode) [82]

$$penicillin + H_2O \xrightarrow{penicillinase} penicillic\ acid + H^+$$

The penicillinase acts as the biocatalyst in the hydrolysis of the penicillin to penicillic acid. This results into a local pH change near the gate region of the ISFET. The output signal helps to determine the amount of penicillin in the sample solution.

The understanding of the ENFET operation is associated with the reaction kinetics of the biological recognition processes and the mass transfer theory.

2.4.1 Enzyme catalyzed reaction of substrate

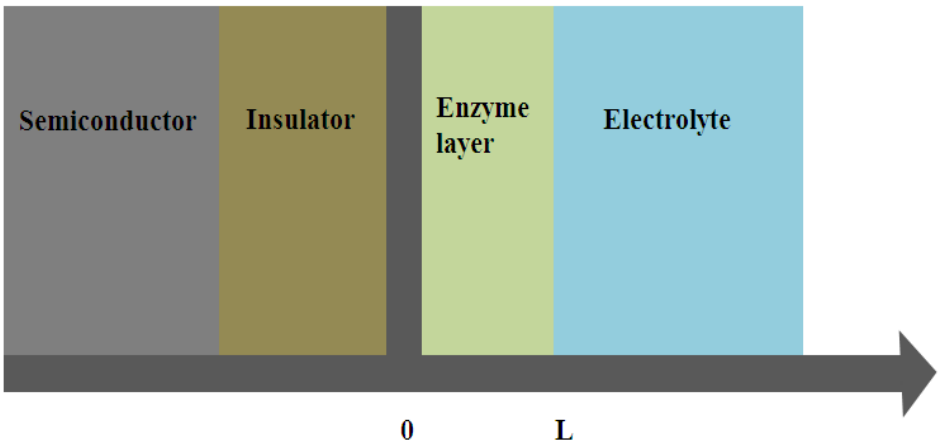

Figure 2.6 Figure illustrating the electrolyte enzyme insulator semiconductor structure

The system is considered to consist of a sensor surface, which is present at x=0 and is coated with an immobilized enzyme layer of thickness L [83]. Beyond this thickness lies the transport boundary layer as illustrated in figure 2.6. The concentration of the analyte, i.e. the substrate S, beyond the transport layer has a defined value [S] and the product concentration [P] is taken as zero. The enzyme catalyzed reaction takes place in the immobilized enzyme layer and it follows the Michaelis Menten kinetics. In this reaction, the substrate is depleted and the product is generated in the enzyme layer. A steady state is reached when the rate of reaction is balanced by the mass transport of reactant and product to and from it.

A single enzyme is considered to be acting on the substrate molecule which follows the Michaelis Menten theory. According to this theory, the enzyme (with concentration E) reacts reversibly with the substrate (with concentration S) to form an enzyme-substrate (ES) complex. Further, the complex breaks apart into product (with concentration P) and the original enzyme and this reaction is irreversible. The overall kinetics is expressed as [60, 83]

$$E+S \underset{k_{-1}}{\overset{k_{+1}}{\rightleftharpoons}} ES \xrightarrow{k_{+2}} E+P$$

The rate of formation of enzyme substrate intermediate is equal to its breakdown.

$$k_{+1}[E][S] = k_{-1}[ES] + k_{+2}[ES]$$

$$[ES] = \frac{k_{+1}[E][S]}{k_{-1} + k_{+2}} \tag{2.43}$$

Combining the three constants gives the Michaelis constant, k_m

$$k_m = \frac{k_{-1} + k_{+2}}{k_{+1}} \tag{2.44}$$

Substituting (2.44) in (2.43)

$$[ES] = \frac{[E][S]}{k_m} \tag{2.45}$$

It is known that,

$$[E] + [ES] = [E_o] \tag{2.46}$$

$[E_o]$ is the total enzyme concentration. Substituting equation (2.46) in (2.45)

$$[ES] = \frac{([E_o] - [ES])[S]}{k_m}$$

$$[ES] = \frac{[E_o][S]}{[S] + k_m} \tag{2.47}$$

The rate at which the product is formed is given by

$$\frac{\delta P}{\delta t} = a = k_{+2}[ES] \tag{2.48}$$

Substituting (2.47) in (2.48)

$$a = k_{+2}\frac{[E_o][S]}{[S]+k_m} \tag{2.49}$$

The maximum value of a, a_{max} is obtained for large value of S_o. Therefore,

$$a_{\max} = k_{+2}[E_o] \tag{2.50}$$

Substituting (2.50) in (2.49)

$$a = a_{\max}\frac{[S]}{[S]+k_m} \tag{2.51}$$

This is the Michaelis Menten equation where a_{max} is the maximal enzyme activity for one enzyme unit. Michaelis constant k_m corresponds to the initial substrate concentration at which the reaction velocity becomes half of its maximum value [60].

2.4.2 Diffusion –reaction equation

The enzyme reaction follows the Michaelis Menten kinetics and the diffusion reaction equation follows the Fick's second law with an extra term which accounts for the consumption or production of a species [60, 84].

$$\frac{\partial C}{\partial t} = D\frac{\partial^2 C}{\partial x^2} \pm R(C) \tag{2.52}$$

D is the diffusion coefficient of the species, $R(C)$ is the reaction term, and the sign indicates whether the species is product or substrate. The reaction term is given by

$$R(x,t) = a_{\max} n_{enz}\frac{[S](x,t)}{[S](x,t)+k_m} \qquad \text{for } 0 \le x \le L \tag{2.53a}$$

$$R(x,t) = 0 \quad \text{for } x > L \tag{2.53b}$$

Using equation (2.52) for the substrate and the product is expressed as

$$\frac{\delta[S](x,t)}{\delta t} = D_S \frac{\delta^2[S](x,t)}{\delta x^2} - R(C) \tag{2.54}$$

$$\frac{\delta[\mathrm{P}](x,t)}{\delta t} = D_P \frac{\delta^2[\mathrm{P}](x,t)}{\delta x^2} + R(C) \tag{2.55}$$

The time derivative is set to zero when steady state response is considered. Therefore,

$$\frac{\delta[S](x,t)}{\delta t} = \frac{\delta[P](x,t)}{\delta t} = 0$$

The solutions can be obtained by considering two limiting cases.

Case 1. $[S] << k_m$, which indicates that the enzyme kinetics is much faster than the transport through the enzymatic layer, the substrate concentration being the limiting factor.

Case 2. $[S] >> k_m$, this represents very high concentration that saturates the enzyme.

For case 1.

Under steady state condition, equation (2.54) becomes

$$D_S \frac{\delta^2[S](x,t)}{\delta x^2} - R(x,t) = 0 \tag{2.56a}$$

$$\text{or} \quad \frac{\delta^2[S](x,t)}{\delta x^2} = \frac{a_{\max} n_{enz}}{D_S} \frac{[\mathrm{S}](\mathrm{x},\mathrm{t})}{[S](x,t) + \mathrm{k}_m} \quad \text{for } 0 \le x \le L \tag{2.56b}$$

Considering $[S] \le k_m$

$$D_S \frac{\delta^2[S](x,t)}{\delta x^2} = a_{\max} n_{enz} \frac{[\mathrm{S}](\mathrm{x},\mathrm{t})}{\mathrm{k}_m} \quad \text{for } 0 \le x \le L$$

$$\frac{\delta^2[S](x,t)}{\delta x^2} = \frac{a_{\max} n_{enz}}{D_S} \frac{[S](x,t)}{k_m}$$

$$\frac{\delta^2[S](x,t)}{\delta x^2} - \alpha[S](x,t) = 0 \qquad (2.57)$$

Where $\alpha = \frac{a_{\max} n_{enz}}{D_S k_m} = \frac{k_{+2}[E_o]}{D_S k_m}$, α is called the enzyme loading factor or diffusion modulus.

The boundary conditions are

$\frac{\delta[S](x,t)}{\delta t} = 0$ at $x = 0$

$[S](x,t) = [S](L,t)$ at $x=L$

$[S](L, t)$ is the substrate concentration at the outer surface of the immobilized enzyme layer at $x=L$. Thus integrating equation (2.57) applying the boundary conditions, the expression obtained is

$$[S](x,t) = \frac{\cosh(x\sqrt{\alpha})}{\cosh(L\sqrt{\alpha})}[S](L,t) \quad \text{for } 0 \le x \le L \qquad (2.58)$$

Here x defines the distance across the enzyme layer, which extends from the interface of enzyme and insulator at $x=0$ to the interface of enzyme and the electrolyte at $x=L$.

Substituting $[S](L, t)$ in equation (2.54) the expression obtained is

$$\frac{\delta[S](L,t)}{\delta t} = -a_{\max} n_{enz} \frac{[S](L,t)}{k_m} \qquad (2.59)$$

Integrating equation (2.59)

$$\ln([S](L,t)) = -\frac{a_{\max} n_{enz} t}{k_m} + C \qquad (2.60)$$

At t=0, $[S](L, t)=S_o$, therefore $C=\ln(S_o)$

$$\ln([S](L,t)) = -\frac{a_{\max} n_{enz} t}{k_m} + \ln(S_o)$$

$$\ln\left(\frac{[S](L,t)}{S_o}\right) = -\frac{a_{\max} n_{enz} t}{k_m}$$

Therefore,

$$[S](L,t) = \exp\left(-\frac{a_{\max} n_{enz} t}{k_m}\right) S_o \tag{2.61}$$

The relationship between substrate and product can be obtained by adding equation (2.54) and (2.55)

$$D_S \frac{\delta^2[S](x,t)}{\delta x^2} + D_P \frac{\delta^2[\mathrm{P}](x,t)}{\delta x^2} = 0 \tag{2.62}$$

Integrating the equation (2.62)

$$D_S \frac{\delta[S](x,t)}{\delta x} + D_P \frac{\delta[\mathrm{P}](x,t)}{\delta x} = constant \quad \text{for } 0 \le x \le L \tag{2.63}$$

At the insulating surface, x=0 the product concentration $[P]_{x=o}=[P_o]$

Integrating equation (2.63)

$$D_S[S](L,t) + D_P[P](L,t) = D_S[S](x,t) + D_p[P](x,t) = constant \tag{2.64}$$

Rearranging equation (2.64) and substituting equation (2.58)

$$D_p[P](x,t) = D_S[S](L,t) - D_S \frac{\cosh(x\sqrt{\alpha})}{\cosh(\mathrm{L}\sqrt{\alpha})}[S](L,t) + D_P[P](L,t) \quad \text{for } 0 \le x \le L$$

$$[P](x,t) = \frac{D_S}{D_p}\left[1 - \frac{\cosh(x\sqrt{\alpha})}{\cosh(\mathrm{L}\sqrt{\alpha})}\right][S](L,t) + [P](L,t) \tag{2.65}$$

At x=0,

$$[P_o] = \frac{D_S}{D_p}\left[1 - \frac{1}{\cosh(L\sqrt{\alpha})}\right][S](L,t) + [P](L,t) \tag{2.66}$$

Substituting $[P](L, t)$ in equation (2.55)

$$\frac{\delta[P](L,t)}{\delta t} = a_{\max} n_{enz} \frac{[S](L,t)}{k_m} \tag{2.67}$$

Integrating equation (2.67) and for t= 0, $[P](L,t)=0$, thus the constant $C= S_o$ therefore, the final expression obtained is

$$[P](L,t) = S_o - \exp\left(\frac{-a_{\max} n_{enz} t}{k_m}\right) S_o \tag{2.68}$$

For the second case: $[S] >> k_m$

$R(x, t)= a_{max}\, n_{enz}$ for $0 \le x \le L$

From equation (2.54)

$$D_S \frac{\delta^2[S](x,t)}{\delta x^2} = a_{\max} n_{enz} \quad \text{for } 0 \le x \le L$$

$$\frac{\delta^2[S](x,t)}{\delta x^2} = \frac{a_{\max} n_{enz}}{D_S} \tag{2.69}$$

Integrating equation (2.69) with the boundary conditions as

$$\frac{\delta[S](x,t)}{\delta t} = 0 \text{ at } x=0 \tag{2.70a}$$

$$[S](x,t) = [S](L,t) \text{ at } x=L \tag{2.70b}$$

The expression obtained is

$$\frac{\delta[S](x,t)}{\delta t} = \alpha' x + C \tag{2.71}$$

Where $\alpha' = \frac{a_{\max} n_{enz}}{D_S}$

Using boundary condition (2.70a), C=0

Integrating the equation (2.71) further after substituting the constant

$$[S](x,t) = \frac{\alpha' x^2}{2} + C_1 \tag{2.72}$$

Using the second boundary equation (2.70b), constant obtained is

$$C_1 = [S](L,t) - \frac{\alpha' L^2}{2}$$

Substituting the constant, equation (2.72) becomes

$$[S](x,t) = [S](L,t) + \frac{\alpha'}{2}\left(x^2 - L^2\right) \quad \text{for } 0 \le x \le L \tag{2.73}$$

Replacing the expression of α' in the equation (2.73)

$$[S](x,t) = [S](L,t) + \frac{a_{\max} n_{enz}}{2D_S}\left(x^2 - L^2\right) \quad \text{for } 0 \le x \le L \tag{2.74}$$

Substituting $[S](L, t)$ in equation (2.54)

$$\frac{\delta[S](L,t)}{\delta t} = -a_{\max} n_{enz} \tag{2.75}$$

On integrating equation (2.75)

$$[S](L,t) = -a_{\max} n_{enz} t + C$$

At $t = 0$, $[S](L, t)=S_o$

$$[S](L,t) = -a_{\max} n_{enz} t + S_o$$

Again from equation (2.64)

$$D_P[P](x,t) = D_S[S](L,t) + D_P[P](L,t) - D_S[S](x,t) \text{ for } 0 \le x \le L$$

$$D_P[P](x,t) = D_S[S](L,t) - D_S[S](x,t) + \frac{a_{\max} n_{enz}}{2D_S}(L^2 - \mathrm{x}^2) + \mathrm{D}_P[P](L,t) \qquad (2.76)$$

Substituting equation (2.74) in (2.76)

$$[\mathrm{P}](\mathrm{x},\mathrm{t}) = [\mathrm{P}](\mathrm{L},\mathrm{t}) + \frac{a_{\max} n_{enz}}{2D_P}(L^2 - x^2) \qquad (2.77)$$

Substituting $[P](L, t)$ in equation (2.55)

$$\frac{\delta[P](L,t)}{\delta t} = a_{\max} n_{enz} \qquad (2.78)$$

Integrating equation (2.78)

$$[P](L,t) = a_{\max} n_{enz} t + C$$

At t=0, [P](L,t)=0

$$[P](L,t) = a_{\max} n_{enz} t$$

For $x>L$

$$\frac{\delta[S](x,t)}{\delta t} = D_S \frac{\delta^2[S](x,t)}{\delta x^2} \qquad (2.79)$$

Assuming steady state

$$\frac{\delta^2[S](x,t)}{\delta x^2} = 0 \tag{2.80}$$

Integrating equation (2.80)

$$\frac{\delta[S](x,t)}{\delta x} = C$$

$$\frac{\delta[S](x,t)}{\delta x} = 0 \text{ at } x=\infty$$

On integration, therefore C=0 the expression obtained

$$[S](x,t) = C$$

At $x=\infty$, $[S](x, t)=S_o$

Therefore, $[S](x, t)=S_o$ for $x > L$

Again,

$$\frac{\delta[P](x,t)}{\delta t} = D_P \frac{\delta^2[P](x,t)}{\delta x^2} \tag{2.81}$$

Assuming steady state,

$$\frac{\delta^2[P](x,t)}{\delta x^2} = 0$$

On integration,

$$\frac{\delta[P](x,t)}{\delta x} = C$$

$$\frac{\delta[P](x,t)}{\delta x} = 0 \text{ at } x=\infty$$

Therefore, C=0

On integration,

$[P](x,t) = C$

At $x = \infty$, $[P](x, t)=0$

Therefore $[P](x, t)=0$ for $x> L$

In other words, the substrate is S_o and product is zero when $x>L$. Further, equation (2.77) the product concentration at the surface (x=0) is a constant that depends on the immobilized enzyme concentration, the reaction kinetics, diffusion mass transport and is independent of the substrate concentration. In this case, since the substrate concentrate is too large that it has saturated the enzyme.

2.5 Results and Discussion

This section presents the general characteristics of ISFET device, simulated using device model, available in the prior literature.

Figure 2.7 shows variation of electrolyte oxide interface potential with pH. In this figure, it can be observed that the electrolyte oxide interface potential varies linearly with pH. Ideal case is considered here therefore β value is taken as unity. At pH below pH_{PZC}, the electrolyte oxide potential is positive and as the pH increases it becomes negative.

Figure 2.8 shows the relationship between drain current (I_{DS}) and drain to source voltage (output characteristics), for different values of pH. From the plot, it is observed that with the change in drain to source voltage (V_{DS}) the current I_{DS} varies. Also, the magnitude of current is higher for lower pH values at same V_{DS}.

Figure 2.9 illustrates the relationship between drain current and gate to source voltage, at different values of pH. This indicates that the threshold voltage of ISFET is a function of pH and hence varies with the change in pH values of the electrolyte.

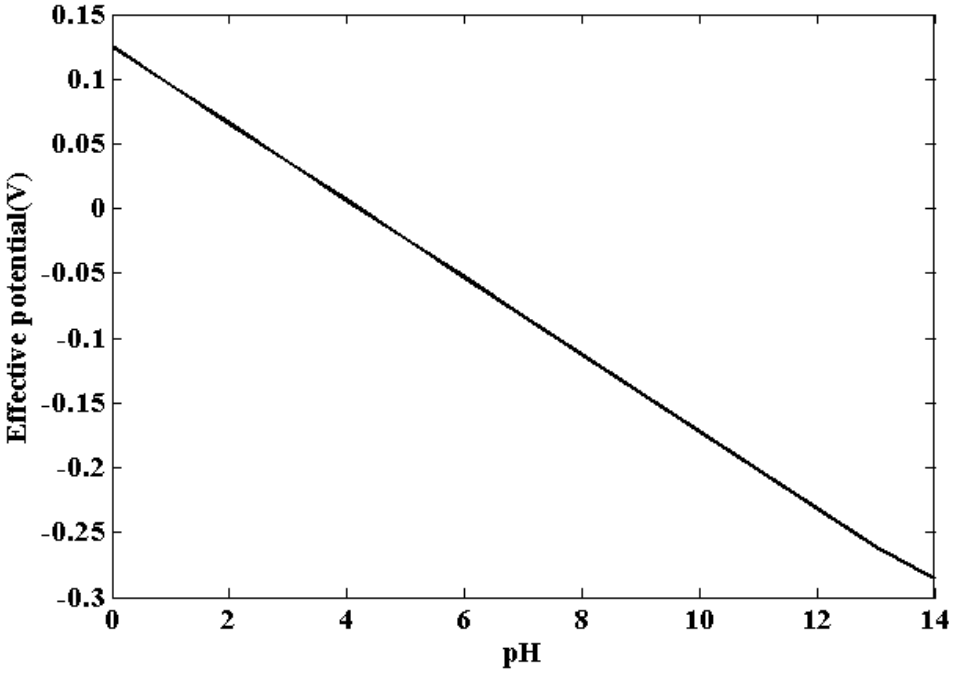

Figure 2.7. Electrolyte oxide interface potential vs. pH for Silicon dioxide

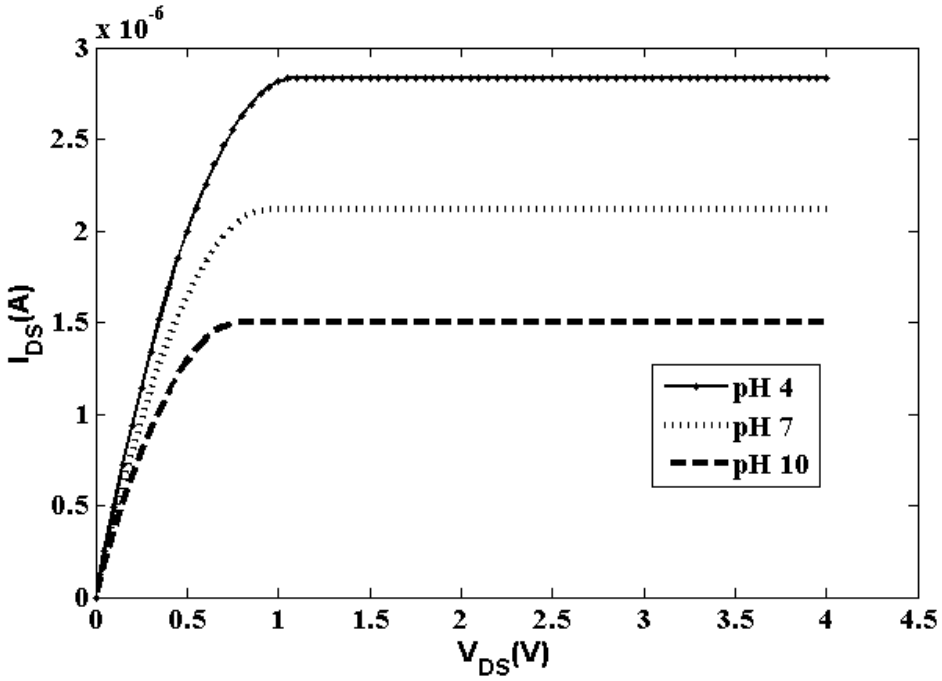

Figure 2.8 Drain Current vs. drain to source voltage at various pH

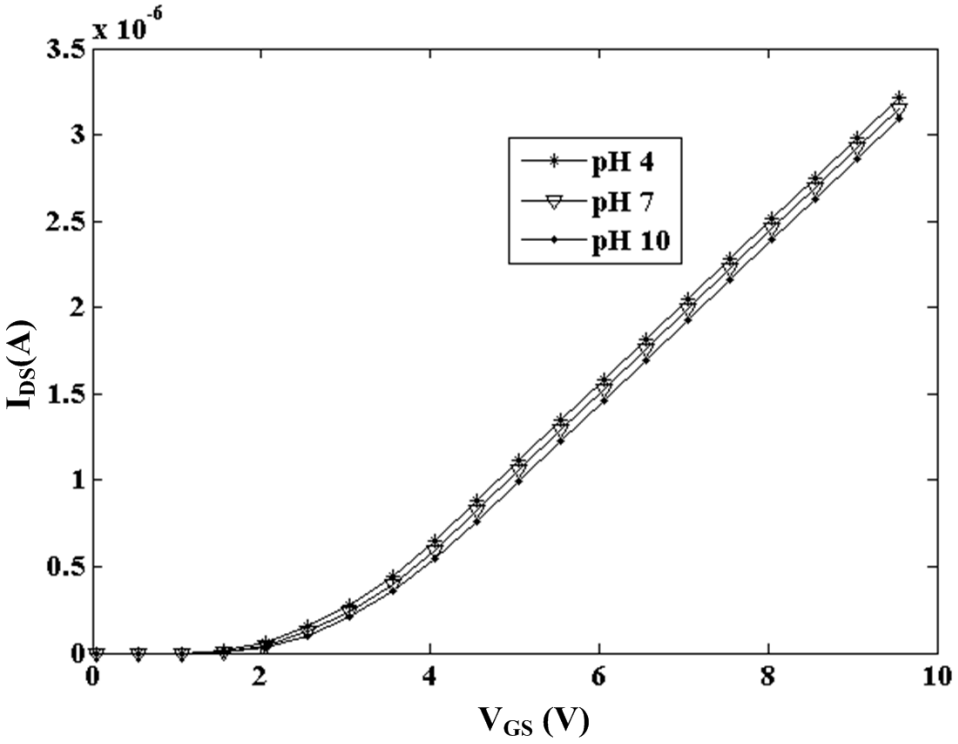

Figure 2.9 Drain Current vs. gate to source voltage at various pH

By the diffusion curves it can be seen that the substrate concentration at the surface of the immobilizing layer is far lower than the product whereas, the product concentration is highest at the surface. This is because the substrate molecule has to diffuse to the immobilizing matrix where they get converted to products.

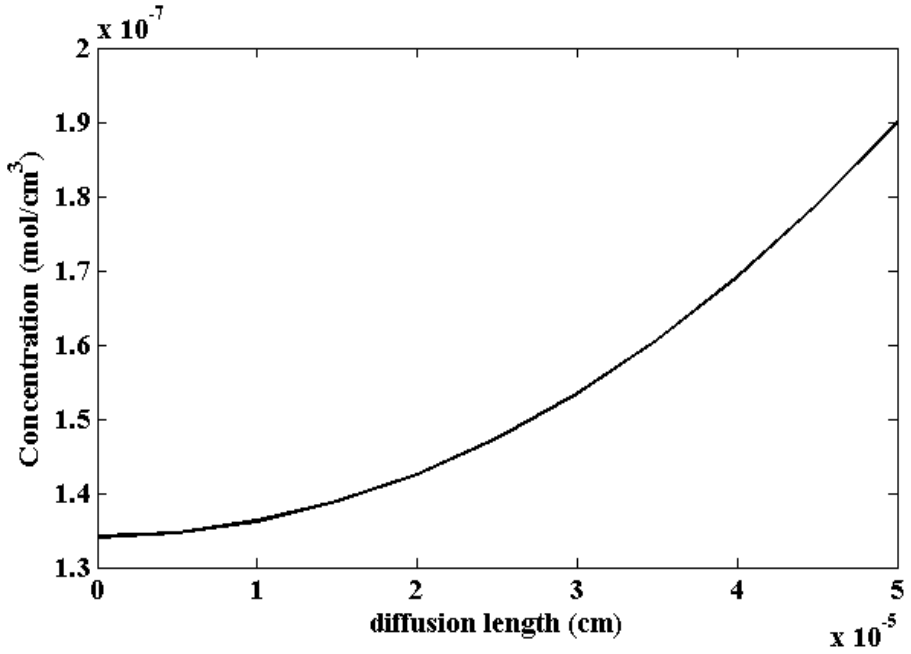

Figure 2.10. Substrate concentration versus diffusion length plot when substrate concentration is less than k_m

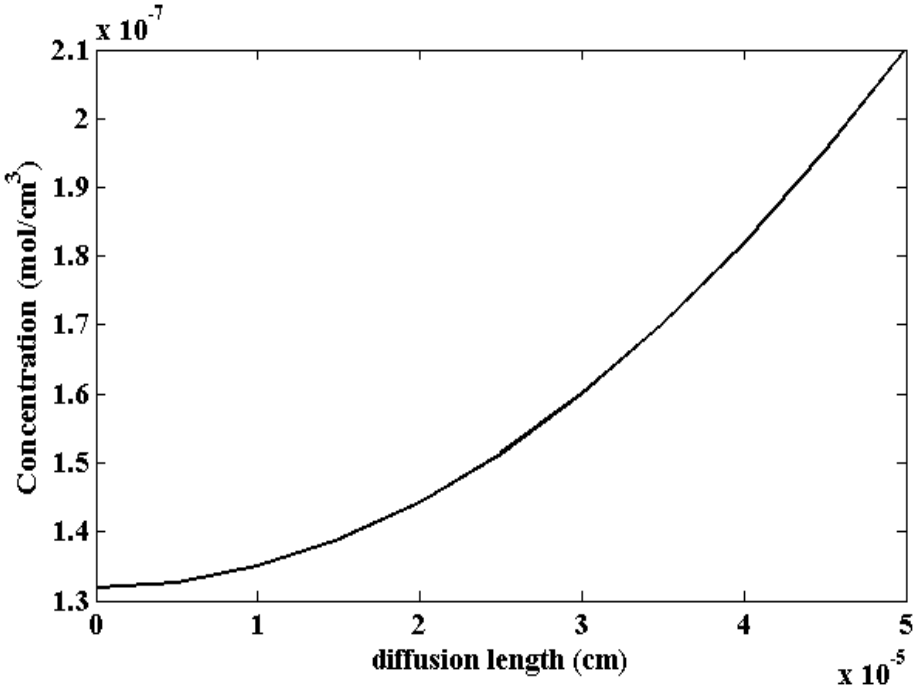

Figure 2.11. Substrate concentration versus diffusion length plot when substrate concentration is greater than k_m

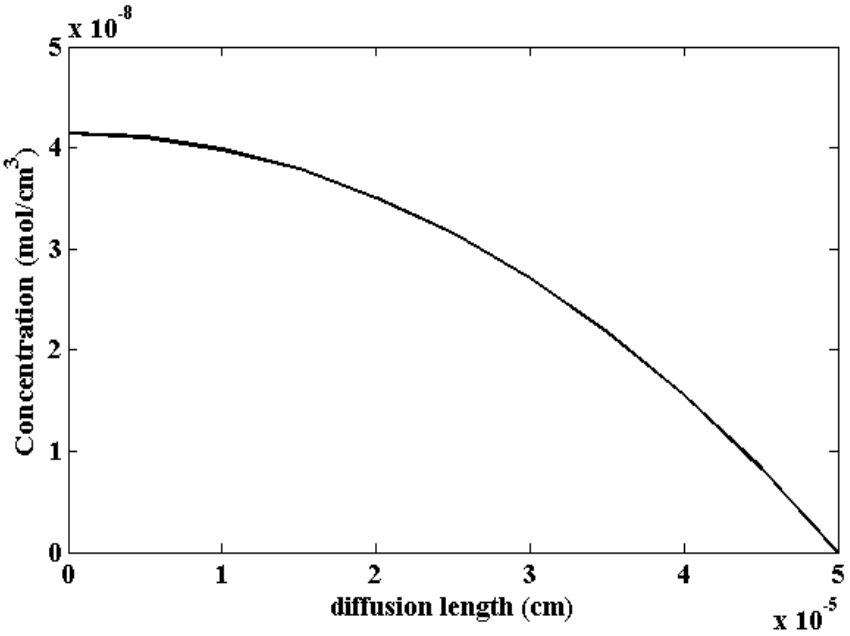

Figure 2.12. Product concentration versus diffusion length plot when substrate concentration is less than k_m

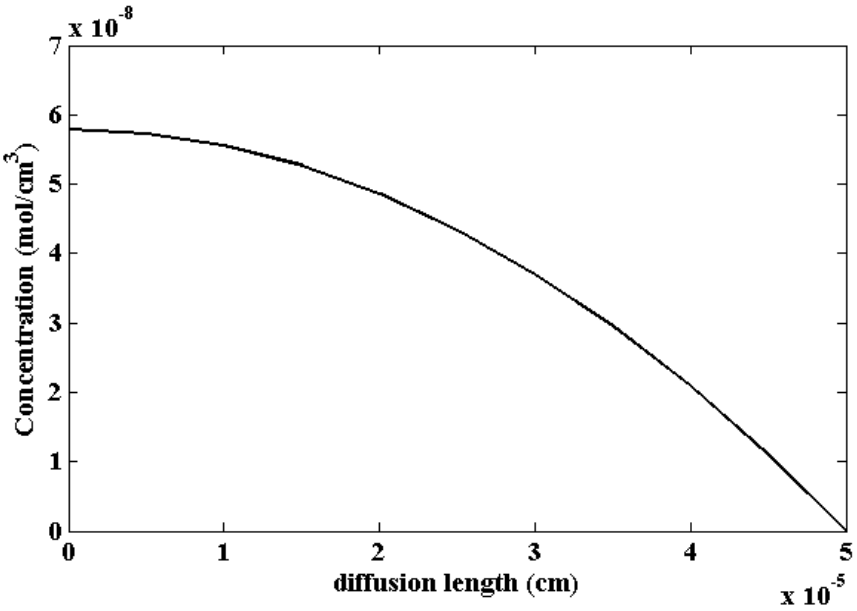

Figure 2.13. Product concentration versus diffusion length plot when substrate concentration is greater than k_m

Data for simulation obtained from [85]:

Substrate concentration: (0.01-0.02) mM

Michaelis Menten constant k_m: 0.2mM

Maximal enzyme activity a_m: 16.67×10^{-9}mol/s

Number of enzymatic units per volume (n_{enz}): 301×10^{4}units/cm^3

Acetylcholine diffusion constant (D_S) 8×10^{-6}cm^2/s

Acetic acid diffusion constant (D_p) 1.08×10^{-5}cm^2/s.

When the substrate concentration is less than the Michaelis constant (k_m), the rate of reaction is faster than the condition when the substrate concentration is higher than k_m. For Substrate concentration lower than k_m (figure 2.10) at maximum diffusion length i.e. at 5×10^{-5} cm, the substrate concentration is 1.9×10^{-7} mol/cm^3 whereas for substrate concentration higher than k_m (figure 2.11) the substrate concentration is 2.1×10^{-7} mol/cm^3. Similar pattern can be seen for the products. When the substrate concentration is lower, the product concentration at the surface is low, which is 4.2×10^{-8} mol/cm^3 (figure 2.12) and for higher substrate concentration the product concentration at the surface is high, which is 5.7×10^{-8} mol/cm^3 as illustrated in figure 2.13.

Bibliography

[1] Middelhoek, S. Celebration of the tenth transducers conference: The past, present and future of transducer research and development. *Sensors and Actuators A: Physical*, 82(1): 2-3, 2000.

[2] Wise, K.D., Angell, J.B., and Starr, A. An integrated-circuit approach to extracellular microelectrodes. *IEEE Transactions on Biomedical Engineering*, 3: 238-247, 1970.

[3] Bergveld, P. New amplification method for depth recording. *IEEE Transactions on Biomedical Engineering*, 2:102-105, 1968.

[4] Bergveld, P. Development of an ion-sensitive solid-state device for neurophysiological measurements. *IEEE Transactions on Biomedical Engineering*, 1:70-71, 1970.

[5] Bergveld, P. Development, operation, and application of the ion-sensitive field-effect transistor as a tool for electrophysiology. *IEEE Transactions on Biomedical Engineering*, 5:342-351, 1972.

[6] Matsuo, T. and Wise, K.D. An integrated field-effect electrode for biopotential recording. *IEEE Transactions on Biomedical Engineering*, 6: 485-487, 1974.

[7] Janata, J. *Principles of chemical sensors*. Plenum Press., New York and London, 1989.

[8] Sandifer, J.R. Theory of interfacial potential differences: effects of adsorption onto hydrated (gel) and nonhydrated surfaces. *Analytical Chemistry*, 60(15):1553-1562, 1988.

[9] Bousse, L., De Rooij, N.F., and Bergveld, P. Operation of chemically sensitive field-effect sensors as a function of the insulator-electrolyte interface. *IEEE Transactions on Electron Devices*, 30(10): 1263-1270, 1983.

[10] Van Der Schoot, B.H., and Bergveld, P. ISFET based enzyme sensors. *Biosensors*, 3(3):161-186, 1987.

[11] Dzyadevych, S.V, Soldatkin, A.P., Anna, V., Martelet, C., and Jaffrezic-Renault, N. Enzyme biosensors based on ion-selective field-effect transistors. *Analytica Chimica Acta*, 568(1-2): 248-258, 2006.

[12]Estrela, P., Stewart, A.G., Yan, F., and Migliorato, P. Field effect detection of biomolecular interactions. *Electrochimica Acta*, 50(25-26): 4995-5000, 2005.

[13] Simonis, A., Dawgul, M., Lüth. H., and Schöning, M.J. Miniaturised reference electrodes for field-effect sensors compatible to silicon chip technology. *Electrochimica Acta*, 51(5):930-937, 2005.

[14] Birrell, S.J. and Hummel, J.W. Real-time multi ISFET/FIA soil analysis system with automatic sample extraction. *Computers and Electronics in Agriculture*, 32(1): 45-67, 2001.

[15] Yuqing, M., Jianrong, C., and Keming, F. New technology for the detection of pH. *Journal of biochemical and biophysical methods*, 63(1):1-9, 2005.

[16] Chen, K.M., Li, G.H., Chen, L.X., and Zhu, Y. Improvement of structural instability of the ion-sensitive field-effect transistor (ISFET). *Sensors and Actuators B: Chemical*, 13(1-3):209-211, 1993.

[17] Harame, D.L., Bousse, L.J., Shott, J.D. and Meindl, J.D. Ion-sensing devices with silicon nitride and borosilicate glass insulators. *IEEE Transactions on Electron Devices*, 34(8):1700-1707, 1987.

[18] Niu, W. Study of Effect of LPCVD Si_3N_4 Films Surface Oxidation on Characteristics of PH-ISFET. *Chinese Journal Of Semiconductors-Chinese Edition*, 14: 317-320, 1993.

[19] Garde, A., Lane, W., and Alderman, J. Improving the Sensitivity of the Si_3N_4 Gate pH-ISFET using Modified Processing Techniques. In *Solid State Device Research Conference* (ESSDERC'94), pages 391-394, 24th European IEEE, 1994.

[20] Te, Y.L., Chou, J.C., Chung, W.C., Sun, T.P., and Hsiung, S.K. Characteristics of silicon nitride after O_2 plasma surface treatment for pH-ISFET applications. *IEEE Transaction on Biomedical Engineering*, 48(3):340–344, 2001.

[21] Moinpour, M., Cheung, P.W., Liao, E., Aw, C.Y., and Weiler, E.B. Chemical response of $Si_3N_4/SiO_2/Si$ structures used in pH microelectronic sensors. In *Engineering in Medicine and Biology Society, Images of the Twenty-First Century.*, Proceedings of the Annual International Conference of the IEEE Engineering, pages 1084-1085, 1989.

[22] Bunjongpru, W., Sungthong, A., Porntheeraphat, S., Rayanasukha, Y., Pankiew, A., Jeamsaksiri, W., Srisuwan, A., Chaisriratanakul, W., Chaowicharat, E., Klunngien, N. and Hruanun, C. Very low drift and high sensitivity of nanocrystal-TiO_2 sensing membrane on pH-ISFET fabricated by CMOS compatible process. *Applied Surface Science*, 267:206-11, 2013.

[23] Jang, H.J., Kim, M.S. and Cho, W.J. Development of Engineered Sensing Membranes for Field-Effect Ion-Sensitive Devices Based on Stacked High-k Dielectric Layers. *IEEE Electron Device Letters*, 32(7): 973-975, 2011.

[24] Pan, T.M. and Liao, K.M. Structural properties and sensing characteristics of Y_2O_3 sensing membrane for pH-ISFET. *Sensors and Actuators B: Chemical*, 127(2):480-485, 2007.

[25] Pan, T.M. and Liao, K.M. Comparison of structural and sensing characteristics of Pr_2O_3 and $PrTiO_3$ sensing membrane for pH-ISFET application. *Sensors and Actuators B: Chemical*, 133(1):97-104, 2008.

[26] Pan, T.M., Lin, J.C., Wu, M.H., and Lai, C.S. Study of high-k Er_2O_3 thin layers as ISFET sensitive insulator surface for pH detection. *Sensors and Actuators B: Chemical*, 138(2):619-624, 2009.

[27] Kaneko, H., Miyake, K., and Teramoto, Y. Electrochemichromism of rf reactively sputtered tungsten-oxide films. *Journal of Applied Physics*, 53(6):4416-4421, 1982.

[28] Chiang, J.L., Chen, Y.C., and Chou, J.C. Simulation and experimental study of the pH-sensing property for AlN thin films. *Japanese Journal of Applied Physics*, 40(10R):5900-5909, 2001.

[29] Bunjongpru, W., Porntheeraphat, S., Trithaveesak, O., Somwang, N., Khomdet, P., Jeamsaksiri, W., Hruanun, C., Poyai, A., and Nukeaw, J. The innovative AlN-ISFET based pH sensor. In *Electrical Engineering/Electronics, Computer, Telecommunications and Information Technology* (ECTI-CON 2008) 5th International Conference, volume 2, pages 833-836, 2008. IEEE.

[30] Shoorideh, K. and Chui, C.O. Optimization of the sensitivity of FET-based biosensors via biasing and surface charge engineering. *IEEE Transactions on Electron Devices*, 59(11):3104-3110, 2012.

[31] Prodromakis, T., Liu, Y., Constandinou, T., Georgiou, P. and Toumazou, C. Exploiting CMOS technology to enhance the performance of ISFET sensors. *IEEE Electron Device Letters*, 31(9):1053-1055, 2010.

[32] Park, J.K., Jang, H.J., Park, J.T., and Cho, W.J. SOI dual-gate ISFET with variable oxide capacitance and channel thickness. *Solid-State Electronics*. 97: 2-7, 2014.

[33] Spijkman, M., Smits, E.C., Cillessen, J.F., Biscarini, F., Blom, P.W., and De Leeuw, D.M. Beyond the Nernst-limit with dual-gate ZnO ion-sensitive field-effect transistors. *Applied Physics Letters*, 98(4):443-502, 2011.

[34] Wunnicke, O. Gate capacitance of back-gated nanowire field-effect transistors. *Applied Physics Letters*, 89(8): 83-102, 2006.

[35] Jimenez-Jorquera, C., Orozco, J., and Baldi, A. ISFET based microsensors for environmental monitoring. *Sensors*, 10(1):61-83, 2009.

[36] Bratov, A., Mun, J., Dominguez, C., and Bartroli, J. Photocurable polymers applied as encapsulating materials for ISFET production. *Sensors and Actuators B: Chemical*, 25(1-3):823-825, 1995.

[37] Janata, J. and Moss, S.D. Chemically sensitive field-effect transistors. *Biomedical engineering*, 11(7): 241-245, 1976.

[38] Caras, S. and Janata, J. Field effect transistor sensitive to penicillin. *Analytical Chemistry*, 52(12): 1935-1937, 1980.

[39] Mulchandani, A. and Rogers, K.R. *Enzyme and microbial biosensors*. Humana Press, Totowa, New Jersey, 1998.

[40] Wan, K., Chovelon, J.M., Jaffrezic-Renault, N. and Soldatkin, A.P. Sensitive detection of pesticide using ENFET with enzymes immobilized by cross-linking and entrapment method. *Sensors and Actuators B: Chemical*, 58(1-3):399-408, 1999.

[41] Lee, C.H., Seo, H.I., Lee, Y.C., Cho, B.W., Jeong, H., and Sohn, B.K. All solid type ISFET glucose sensor with fast response and high sensitivity characteristics. *Sensors and Actuators B: Chemical*, 64(1-3):37-41, 2000.

[42] Park, K.Y., Lee, M., and Sohn, B.K. Improved recovery characteristics of ISFET glucose sensor using electrolysis method. *Electronics Letters*, 37(8):495-497, 2001.

[43] Park, K.Y., Choi, S.B., Lee, M., Sohn, B.K., and Choi, S.Y. ISFET glucose sensor system with fast recovery characteristics by employing electrolysis. *Sensors and Actuators B: Chemical*, 83(1-3):90-97, 2002.

[44] Poghossian, A., Yoshinobu, T., Simonis, A., Ecken, H., Lüth, H. and Schöning, M.J. Penicillin detection by means of field-effect based sensors: EnFET, capacitive EIS sensor or LAPS?. *Sensors and Actuators B: Chemical*, 78(1-3):237-242, 2001.

[45] Gorchkov, D.V., Soldatkin, A.P., Maupas, H., Martelet, C., and Jaffrezic-Renault, N. Correlation between the electrical charge properties of polymeric membranes and the characteristics of ion field effect transistors or penicillinase based enzymatic field effect transistors. *Analytica chimica acta*, 331(3):217-223, 1996.

[46] Simonian, A.L., Grimsley, J.K., Flounders, A.W., Schoeniger, J.S., Cheng, T.C., DeFrank, J.J., and Wild, J.R. Enzyme-based biosensor for the direct detection of fluorine-containing organophosphates. *Analytica chimica acta*, 442(1):15-23, 2001.

[47] Zayats, M., Kharitonov, A.B., Katz, E., Bückmann, A.F., and Willner, I. An integrated NAD^+-dependent enzyme-functionalized field-effect transistor (ENFET) system: development of a lactate biosensor. *Biosensors and Bioelectronics*, 15(11-12):671-680, 2000.

[48] Kharitonov, A.B., Zayats, M., Alfonta, L., Katz, E., and Willner, I. A novel ISFET-based NAD^+-dependent enzyme sensor for lactate. *Sensors and Actuators B: Chemical*, 76(1-3):203-210, 2001.

[49] Sandifer, J.R., and Voycheck, J.J. A review of biosensor and industrial applications of pH-ISFETs and an evaluation of Honeywell's "DuraFET". *Microchimica Acta*, 131(1-2): 91-98, 1999.

[50] Dzyadevich, S.V., Korpan , Y.I., Arkhipova, V.N., Alesina, M.Y., Martelet, C., Anna, V., and Soldatkin, A.P. Application of enzyme field-effect transistors for determination of glucose concentrations in blood serum. *Biosensors and Bioelectronics*, 14(3):283-287, 1999.

[51] Poghossian, A.S. Method of fabrication of ISFET-based biosensors on an Si–SiO_2–Si structure. *Sensors and Actuators B: Chemical*, 44(1-3):361-364, 1997.

[52] Gorchkov, D.V., Poyard, S., Soldatkin, A.P., Jaffrezic-Renault, N., and Martelet, C. Application of the charged polymeric materials as additional permselective membranes for improvement of the performance characteristics of urea-sensitive ENFETs . Urea determination in blood serum. *Materials Science and Engineering: C*, 5(1):29-34, 1997.

[53] Boubriak, O.A., Soldatkin, A.P., Starodub, N.F., Sandrovsky, A.K., and El'skaya, A.K. Determination of urea in blood serum by a urease biosensor based on an ion-sensitive field-effect transistor. *Sensors and Actuators B: Chemical*, 27(1-3):429-431, 1995.

[54] Pijanowska, D.G. and Torbicz, W. pH-ISFET based urea biosensor. *Sensors and Actuators B: Chemical*, 44(1-3): 370-376, 1997.

[55] Soldatkin, A.P., Montoriol, J., Sant, W., Martelet, C., and Jaffrezic-Renault, N. Creatinine sensitive biosensor based on ISFETs and creatinine deiminase immobilised in BSA membrane. *Talanta*. 58(2):351-357, 2002.

[56] Volotovsky, V. and Kim, N. Ascorbic acid determination with an ion-sensitive field effect transistor-based peroxidase biosensor. *Analytica chimica acta*, 359(1-2):143-148, 1998.

[57] Kullick, T., Bock, U., Schubert, J., Scheper, T., and Schügerl, K. Application of enzyme-field effect transistor sensor arrays as detectors in a flow-injection analysis system for simultaneous monitoring of medium components. Part II. Monitoring of cultivation processes. *Analytica chimica acta*, 300(1-3):25-31, 1995.

[58] Liu, J., Liang, L., Li, G., Han, R., and Chen, K. H^+ ISFET-based biosensor for determination of penicillin G. *Biosensors and Bioelectronics*, 13(9):1023-1028, 1998.

[59] Bergveld, P. Thirty years of ISFETOLOGY: What happened in the past 30 years and what may happen in the next 30 years. *Sensors and Actuators B: Chemical*, 88(1):1-20, 2003.

[60] Grattarola , M. and Giuseppe, M. *Bioelectronics Handbook*, McGraw Hill, 1998.

[61] Yates, D.E., Levine, S., and Healy, T.W. Site-binding model of the electrical double layer at the oxide/water interface. *Journal of the Chemical Society, Faraday Transactions 1: Physical Chemistry in Condensed Phases*, 70:1807-1818, 1974.

[62] Fung, C.D., Cheung, P.W., and Ko, W.H. A generalized theory of an electrolyte-insulator-semiconductor field-effect transistor. *IEEE Transactions on Electron Devices*, 33(1): 8-18, 1986.

[63] Siu, W.M. Basic properties of the electrolyte—SiO_2—Si system: physical and theoretical aspects. *IEEE Transactions on Electron Devices*, 26(11): 1805-1815, 1979.

[64] Gouy, M. Sur la constitution de la charge électrique à la surface d'un électrolyte. *Journal of Physics Theoretical Application*, 9(1): 457-468, 1910.

[65] Chapman, D. L. LI. A contribution to the theory of electrocapillarity. *The London, Edinburgh, and Dublin philosophical magazine and journal of science*, 25(148): 475-481, 1913.

[66] Stern, O. The theory of the electrolytic double-layer. *Zournal of Elektrochemistry*, 30(508): 1014-1020, 1924.

[67] Grahame, D.C. The electrical double layer and the theory of electrocapillarity. *Chemical reviews*, 41(3):441-501, 1947.

[68] Sharma, S. *Modeling and Simulation of nanobioelectronic device the cylindrical ion sensitive field effect transistor*, PhD Thesis, Department of Electronics and Communication Engineering, Tezpur University, Tezpur, India, 2009

[69] Massobrio, G., Martinoia, S. and Grattarola, M. Use of SPICE for modeling silicon-based chemical sensors. *Sensors and Materials*, 6(2): 101-106, 1994.

[70] Bergveld, P., Van Hal, R.E., and Eijkel, J.C. The remarkable similarity between the acid-base properties of ISFETs and proteins and the consequences for the design of ISFET biosensors. *Biosensors and Bioelectronics*, 10(5):405-414, 1995.

[71] Van Hal, R.E., Eijkel, J.C., and Bergveld, P. A novel description of ISFET sensitivity with the buffer capacity and double-layer capacitance as key parameters. *Sensors and Actuators B: Chemical*, 24(1-3):201-205, 1995.

[72] Van Hal, R.E., Eijkel, J.C., and Bergveld, P. A general model to describe the electrostatic potential at electrolyte oxide interfaces. *Advances in colloid and interface science*, 69(1-3): 31-62, 1996.

[73] Dutta, J.C. Ion sensitive field effect transistor for applications in bioelectronic sensors: a research review. In *Computational Intelligence and Signal Processing (CISP)*, 2012 2nd National Conference on 2012, pages 185-191, Mar 2, 2012.

[74] Fung, C.D., Cheung, P.W., and Ko, W.H. A generalized theory of an electrolyte-insulator-semiconductor field-effect transistor. *IEEE Transactions on Electron Devices*, 33(1):8-18, 1986.

[75] Dousma, J. *A colloidal chemical study of the formation of iron oxyhydroxide*. PhD Thesis , R ijksuniversiteit te Utrecht, Utrecht, 1979.

[76] Healy, T.W., Yates, D.E., White, L.R., and Chan, D. Nernstian and non-Nernstian potential differences at aqueous interfaces. *Journal of Electroanalytical Chemistry and Interfacial Electrochemistry*, 80(1):57-66, 1977.

[77] Schöning, M.J. and Poghossian, A. Recent advances in biologically sensitive field-effect transistors (BioFETs). *Analyst*, 127(9): 1137-1151, 2002.

[78] Clark, L.C. and Lyons, C. Electrode systems for continuous monitoring in cardiovascular surgery. *Annals of the New York Academy of sciences*, 102(1):29-45, 1962.

[79] Janata, J. *Solid state chemical sensors*. Academic Press, 2012.

[80] Thévenot, D.R., Toth, K., Durst, R.A., and Wilson, G.S. Electrochemical biosensors: recommended definitions and classification. *Biosensors and Bioelectronics*, 16(1):121-131, 2001.

[81] Hall, E.A. *Biosensors*, Open University Press, Milton Keynes, England, 1990.

[82] Poghossian, A., Schöning, M.J., Schroth , P. , Simonis, A., and Lüth, H. An ISFET-based penicillin sensor with high sensitivity, low detection limit and long lifetime. *Sensors and Actuators B: Chemical*, 76(1): 519-526, 2001.

[83] Roy, B., Sharma, S., Medhi, T., and Sarma, D.J. Modeling the transient and steady state behaviour of a Glucose Oxidase based enzyme field effect

transistor. In *2015 International Conference on Electrical, Electronics, Signals, Communication and Optimization (EESCO)*, Jan 24, 2015.

[84] Caras, S.D. and Janata, J. pH-based enzyme potentiometric sensors. Part 3. Penicillin-sensitive field effect transistor. *Analytical chemistry*, 57(9):1924-1925, 1985.

[85] Sharma, P.K., Thakur, H.R., and Dutta, J.C. Modeling and simulation of carbon nanotube-based dual-gated enzyme field effect transistor for acetylcholine detection. *Journal of Computational Electronics*, 16:1-9, 2017.